ECCOMAS Congress 2016
VII European Congress on Computational Methods in Applied Sciences and Engineering
M. Papadrakakis, V. Papadopoulos, G. Stefanou, V. Plevris (eds.)
Crete Island, Greece, 5–10 June 2016

# XFEM ANALYSIS – INCLUDING BUCKLING – OF COMPOSITE SHELLS CONTAINING DELAMINATION

**Wilhelm J.H. Rust**[1], **Saleh Yazdani**[2], **and Peter Wriggers**[2]

[1] Hochschule Hannover – University of Applied Sciences and Arts, Ricklinger Stadtweg 120, 30459 Hannover, Germany
wilhelm.rust@hs-hannover.de

[2] Institute of Continuum Mechanics, Leibniz Universität Hannover, Appelstraße 11, 30167 Hannover, Germany
e-mails: yazdani@ikm.uni-hannover.de; wriggers@ikm.uni-hannover.de

**Keywords:** XFEM, Delamination, Shells, Buckling.

**Abstract.** *Based on a first-order shear-deformation theory a four-noded shell element is formulated for composite laminates with and without a delamination. Interlaminar stresses are calculated to evaluate a delamination criterion. The presentation will show how and how accurate. Once the danger of delamination is detected the displacement field is enriched in the sense of the eXtended FEM to account for a discontinuity at an arbitrary position. The remaining strength after starting delamination is simulated by a mixed-mode cohesive zone model based on energy release. Contact when reclosing a discontinuity is included. Large rotations are covered by Green's strain.*

*The developed formulation is tested for shell problems by comparing its results with available benchmark tests for in- and out-of-plane load cases. The feasibility and practicality of the presented model and its advantage over the approach using two shell elements at the predefined plane of the discontinuity, connected by a third one, a cohesive zone element, is demonstrated. Then, linear and non-linear buckling analyses for composite laminates containing a delamination are performed. It is shown how imperfections of the delamination type, i.e. concerning the discontinuity, used for non-linear analysis are based on the modes from linear buckling.*

*The full process from starting with one layer of elements over detecting a delamination to simulating its growth and its interaction with buckling is outlined.*

## 1 INTRODUCTION

When modeling delamination this can be done with two shell or solid elements over each other where all the interface area is bonded but the delaminated region. In such a model delamination propagation can be accounted for by a fracture criterion or a stress criterion in bonded contact, residual strength by a cohesive zone element. However, this requires double elements for the continuous region, too. Furthermore, if the delamination can appear between arbitrary layers not known before starting the analysis *n* thin solid elements and *n*-1 cohesive zones above each other are needed leading to enormous model sizes.

In the present formulation, the discontinuity can be activated at any region of interest without extra simulation effort. To do so, shape functions are enriched by defining extra degrees of freedom (DOF), holding the property of the partition of unity [1]. Thus, the behaviour of the discontinuous subdomains is described using these DOFs. A flat-shell formulation based on a First-order Shear Deformable Theory (FSDT) is developed. The proposed model is implemented in the finite element method using four-noded elements. Due to the robustness and simplicity of lower-order theories in the non-linear simulations [2], in the present formulation the XFEM topology and the geometrically non-linear terms can be effectively combined. The shell formulation is verified for a benchmark test problem of shells in non-linear regime. Then, several numerical tests are carried out for the linear and non-linear delamination buckling analyses of composite laminates. More tests an details are published in [8]. In the next section, the formulation is briefly described.

## 2 FORMULATION

All the formulations are developed with respect to the local Cartesian coordinate system which is located on each flat element. Later, a transformation from local to the global Cartesian coordinate system is required to include the coupling between membrane and bending components of shell structures [3, 4].

### 2.1 Discontinuous flat-shell element

The first-order displacement field in the local Cartesian coordinate system is enriched by XFEM as follows:

$$\begin{aligned} U(x,y,z) &= u^0(x,y) + H(z_d)a_u^0(x,y) + z\left(\theta_y^0(x,y) + H(z_d)a_{\theta_y}^0(x,y)\right) \\ V(x,y,z) &= v^0(x,y) + H(z_d)a_v^0(x,y) - z\left(\theta_x^0(x,y) + H(z_d)a_{\theta_x}^0(x,y)\right) \\ W(x,y,z) &= w^0(x,y) + H(z_d)a_w^0(x,y) \end{aligned} \tag{1}$$

where $u^0$, $v^0$, $w^0$, $\theta_x^0$, and $\theta_y^0$ are the normal DOFs while $a_u^0$, $a_v^0$, $a_w^0$, $a_{\theta_x}^0$, and $a_{\theta_y}^0$ are associated to the enriched DOFs. The superscript 0 indicates the middle plane kinematic variables. $H(z_d)$ is the Heaviside function, let it be $H^*$, shifted by $z_d$ which gets values zero and one below and above the discontinuous surface, respectively:

$$H(z_d) := H^*(z - z_d) = \begin{cases} 1 & for\ z > z_d \\ 0 & for\ z \le z_d \end{cases}$$

This function is being used to activate the extra DOFs when they are required. Therefore, two subdomains ($\Omega^-$ and $\Omega^+$) are identified by $z_d$, being the location of delamination in the thickness direction. The introduced discontinuous element and subdomains are shown in Figure 1.

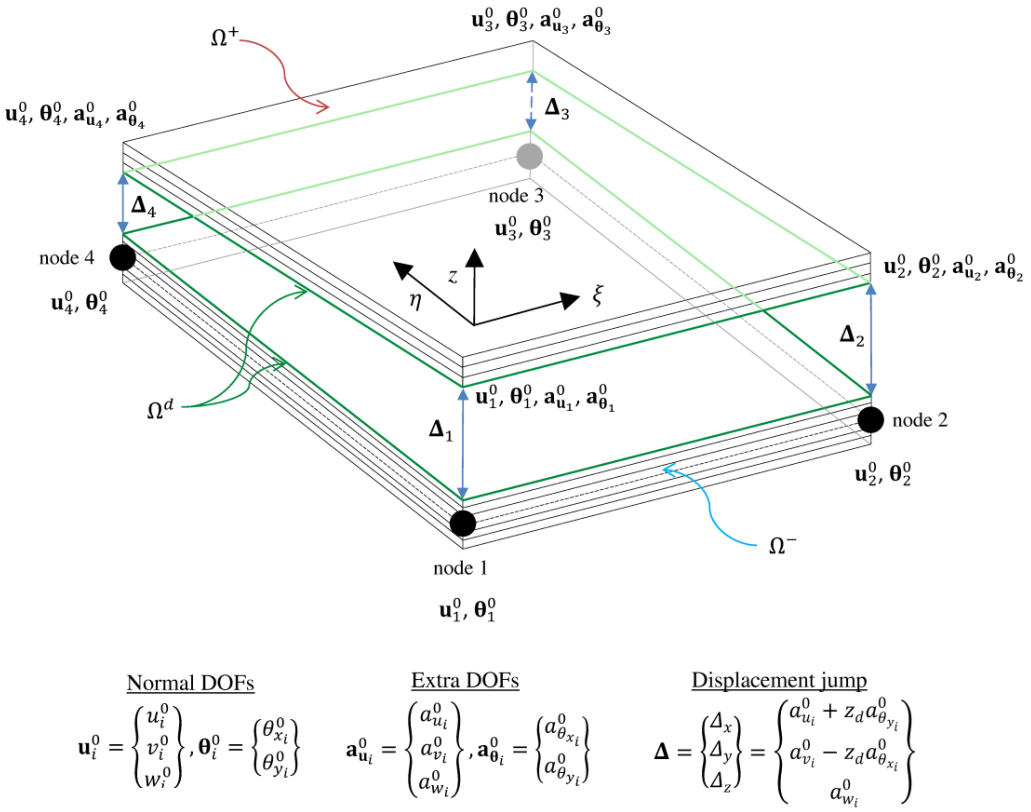


Figure 1: A discontinuous XFEM element.

By inserting the proposed displacement field into the Green-strain tensor and considering the quadratic terms associate to the in-plane components, the strain field is calculated as

$$
\begin{aligned}
\varepsilon_x &= u_{,x}^0 + z\theta_{y,x}^0 + H(z_d)\left(a_{u,x}^0 + z a_{\theta_y,x}^0\right) + \frac{1}{2}\left(u_{,x}^0 + H(z_d)a_{u,x}^0\right)^2 + \frac{1}{2}\left(v_{,x}^0 + H(z_d)a_{v,x}^0\right)^2 + \frac{1}{2}\left(w_{,x}^0 + H(z_d)a_{w,x}^0\right)^2 \\
\varepsilon_y &= v_{,y}^0 - z\theta_{x,y}^0 + H(z_d)\left(a_{v,y}^0 - z a_{\theta_x,y}^0\right) + \frac{1}{2}\left(u_{,y}^0 + H(z_d)a_{u,y}^0\right)^2 + \frac{1}{2}\left(v_{,y}^0 + H(z_d)a_{v,y}^0\right)^2 + \frac{1}{2}\left(w_{,y}^0 + H(z_d)a_{w,y}^0\right)^2 \\
\gamma_{xy} &= \left(u_{,y}^0 + H(z_d)a_{u,y}^0\right) + \left(v_{,x}^0 + H(z_d)a_{v,x}^0\right) + z\left(\theta_{y,y}^0 + H(z_d)a_{\theta_y,y}^0\right) - z\left(\theta_{x,x}^0 + H(z_d)a_{\theta_x,x}^0\right) + \\
&\left(u_{,x}^0 + H(z_d)a_{u,x}^0\right)\left(u_{,y}^0 + H(z_d)a_{u,y}^0\right) + \left(v_{,x}^0 + H(z_d)a_{v,x}^0\right)\left(v_{,y}^0 + H(z_d)a_{v,y}^0\right) + \left(w_{,x}^0 + H(z_d)a_{w,x}^0\right)\left(w_{,y}^0 + H(z_d)a_{w,y}^0\right) \\
\gamma_{xz} &= w_{,x}^0 + \theta_y^0 + H(z_d)\left(a_{w,x}^0 + a_{\theta_y}^0\right) \\
\gamma_{yz} &= w_{,y}^0 - \theta_x^0 + H(z_d)\left(a_{w,y}^0 - a_{\theta_x}^0\right)
\end{aligned}
\tag{2}
$$

The higher-order terms in Eq. (2) are utilized to capture the large deflection response of the laminates. By substituting the acquired strain field into the constitutive equation of orthotropic materials, the stress field is acquired. Due to the lack of parabolic distribution of transverse shear stresses in this theory, the so-called shear correction factor is calculated. In addition, since the formulation is based on a lower-order approach which shows locking for very thin laminates, the shear strain field has been replaced by an assumed one.

The principle of virtual work is applied to obtain the governing equations. To achieve a quadratic convergence in the context of the Newton-Raphson algorithm, the obtained formulations should be linearized with respect to all normal and enriched unknowns [2, 7]. A transformation from the local Cartesian coordinate system to the global one has been performed to

form the flat elements on the curved surface. This transformation is based on the standard procedure using four rotational matrices (in XFEM formulation eight rotational matrices) explained by Zienkiewicz and Taylor in Ref. [4]. Henceforth, owing to the transformation into the curve surface the coupling between membrane and bending components are formed as well as two extra variables, being the drilling DOFs. One of the drilling variables belongs to the finite element part of the problem whereas the other one corresponds to the XFEM.

### 2.2 Drilling degrees of freedom

To avoid the singularity which is faced in the solution process of co-planar elements due to missing stiffness related to drilling dofs pointing out of plane, the penalty method is implemented[4]. In this case, the rotational stiffness coefficient is related to the membrane stiffness components in such a manner that the overall equilibrium equation is not disturbed. Therefore, the drilling potential energy, containing a penalty parameter, is defined as

$$\Pi_{drilling} = \frac{1}{2}\int_{\Omega} P\left(\omega^0 - \theta_z^0\right)^2 d\Omega \tag{3}$$

where $P$ is the penalty parameter, $\theta_z^0$ is the drilling degree of freedom, and $\omega$ is the in-plane rotation of the shell which is related to the membrane DOFs as follows

$$\omega^0 = \frac{1}{2}\left(v_{,x}^0 - u_{,y}^0\right) \tag{4}$$

The amplitude of the penalty parameter can be chosen as $P=10^{-4}E_1h$. The stiffness which is driven based on the presented potential energy can be included for all elements whether they are co-planar or not. It is of importance to conquer the singularity by the aforementioned methods in the local Cartesian coordinate system before the transformation into the global coordinate system.

### 2.3 Contact formulation

In the linear buckling analysis, it is possible to obtain a few mode shapes concerning the penetration of discontinuous surfaces. Though, these mode shapes cannot be physically interpreted. In addition, performing the non-linear analysis may lead to the overlaps between contact subdomains in the post-buckling regime. Therefore, a simple contact formulation based on the penalty method has been taken into account. The relative displacements at the interface region can be simply calculated through the enhanced DOFs in where the contact force values are retrieved as

$$F_c = P\delta_z \tag{5}$$

where $F_c$ is the contact force, $P$ is the penalty stiffness value, and $\delta_z$ is the gap between the subdomains. Once the overlapping of the subdomains lead to negative values for the relative displacement $\delta_z$ during the non-linear buckling analysis, the above formulation is activated and the contact forces hold the equilibrium at the contact area. It is noted that the penalty stiffness value should be chosen sufficiently high to ensure a perfect bonding at the interface region.

All the developed formulations are set up as a user element routine in ANSYS 14.5 commercial software. In the next section, some numerical case studies are carried out based on the developed formulation.

## 3 NUMERICAL TESTS

In this section numerical tests are carried out to verify the accuracy of the XFEM model in predicting the structural response of composite laminates containing the delamination. In addition, convergence studies are performed to check the precision of the formulation. The material properties of studied laminates are given in Table 1.

| Type | $E_{11}$ | $E_{22}$ | $\nu_{12}$ | $G_{12}$ | $G_{13}$ | $G_{23}$ |
|---|---|---|---|---|---|---|
| Shell [5] | 3300 Pa | 1100 Pa | 0.3 | 660 Pa | 660 Pa | 660 Pa |
| Plate [6] | 142 GPa | 10.8 GPa | 0.3 | 5.49 GPa | 5.49 GPa | 3.72 GPa |

Table 1: Material properties of studied laminates.

### 3.1 Nonlinear static analysis

The three layers cross-ply [0°/90°/0°] and [90°/0°/90°] cylindrical panels are analysed. The dimensions of the shell are: $L$=508 m, $R$=2540 m, and $\phi$=0.1 rad. The shell is supposed to be hinged at the edges along the axial direction while it is free on the other edges. Two different thicknesses $h_1$=6.35 m and $h_2$=12.7 m are modelled and they are subjected to an external point load at the centre. Due to the symmetry, only a quarter of the shell is simulated. A schematic view of the shell is shown in Figure 2.

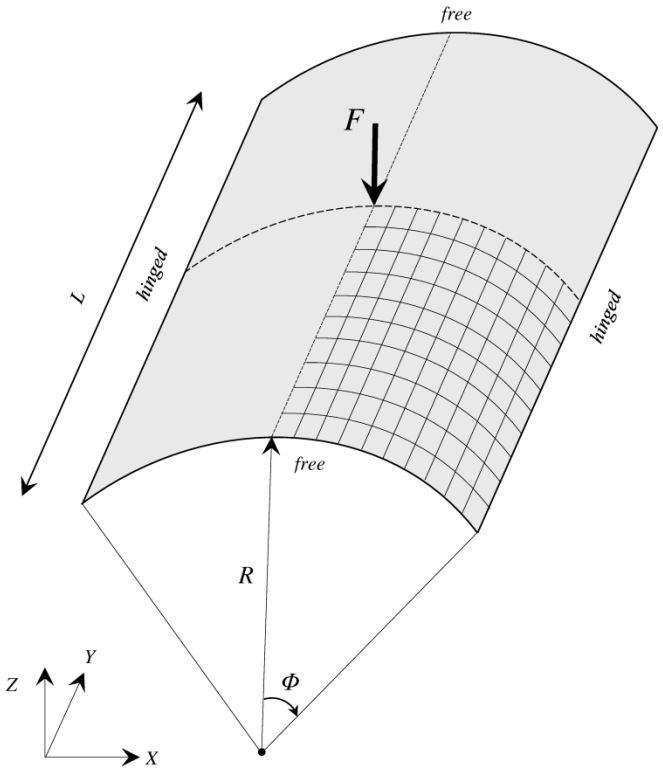


Figure 2: The schematic view of the hinged cylindrical shell.

In order to precisely track the response of the laminate under the applied load, arc-length solution available in ANSYS software is activated. The load versus transverse displacement response of the laminates at the point where the load is applied is depicted in Figure 3.

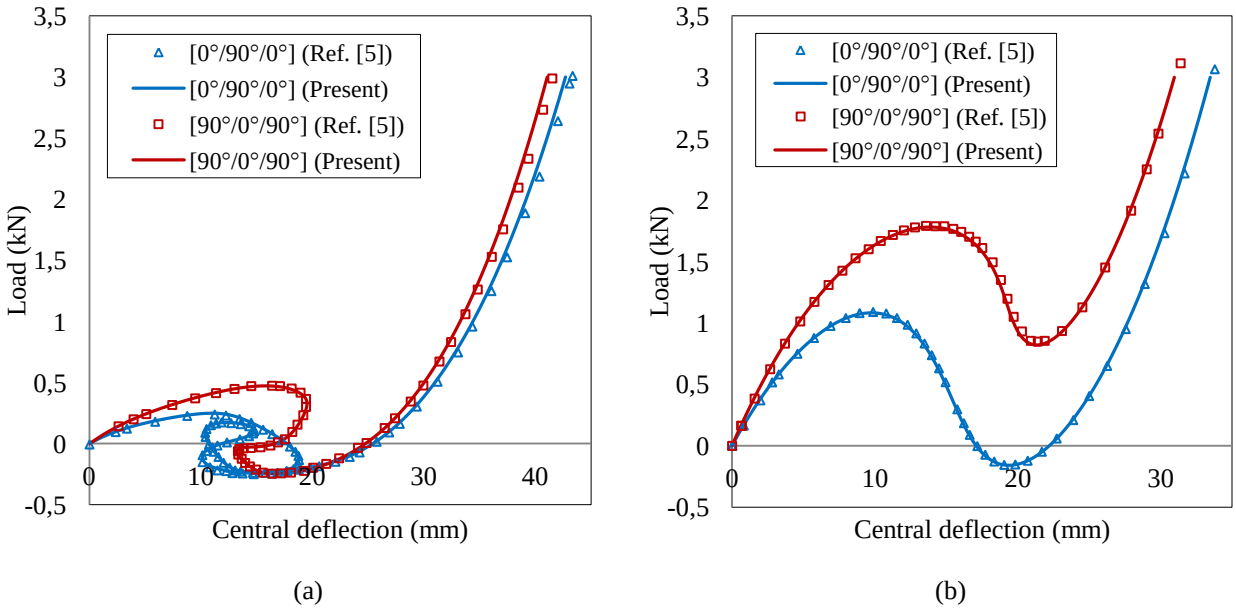


Figure 3: Load-deflection response of the cylindrical shell: (a) $h$=6.35 m; (b) $h$=12.7 m.

As it is shown in Figure 3, the results agree very well with the ones reported in Ref [5].

### 3.2 Delamination buckling analysis

Next, the buckling analysis of multi-layered laminated plate $[45°/-45°/0°/90°]_s$ is investigated. The dimensions of the plate are $a$=0.5 m, $b$=0.025 m, and $h$=0.001 m where a delamination of length $t$ is inserted exactly in the middle of the thickness, between the fourth and fifth layers. The plate is considered as fully clamped on one of the small edges whereas subjected to axial compressive load on the other small edge. The schematic view of the studied laminate is shown in Figure 4.

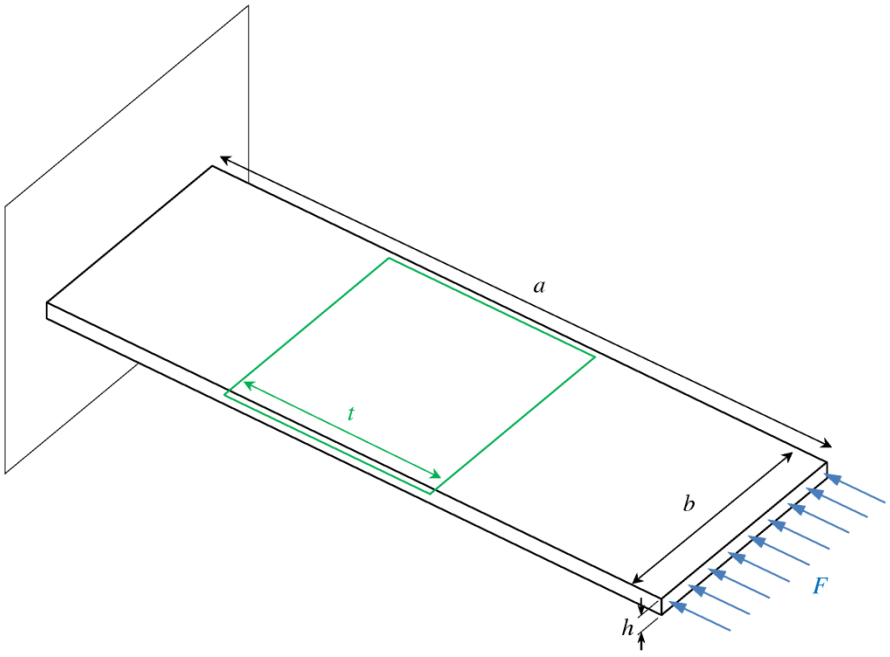


Figure 4: Schematic view of the delaminated composite plate.

In the simulation process of the continuous part, only the normal degrees of freedom are considered. However, extra degrees of freedom are activated in where the discontinuous region exists. To survey the precision of the XFEM model developed, a convergence study on the linear buckling analysis of composite laminate with the delamination length $t$=40 mm is carried out.

For the linear buckling analysis, the tangent stiffness matrix can be split up into linear and non-linear parts. Therefore, the tangent operator $\mathbf{K}_T$ can be written as

$$\mathbf{K}_T = \mathbf{K}_L + \mathbf{K}_U + \mathbf{K}_\sigma \tag{6}$$

where $\mathbf{K}_L$ is the linear stiffness matrix, $\mathbf{K}_U$ is the non-linear part of the stiffness matrix which is related to the initial deformation, and $\mathbf{K}_\sigma$ is the other non-linear part which is the so-called geometric stiffness matrix or initial stress matrix, in case of a Green-strain formulation not directly depending on the displacements, only via the stress. Hence, the linear eigenvalue analysis can be formulated as follows [7]

$$\left(\mathbf{K}_L + \lambda_i \left(\mathbf{K}_\sigma\right)\right)\phi_i = \mathbf{0} \tag{7}$$

where $\lambda_i$ is the critical load factor whereas $\Phi_i$ is the corresponding mode shape. The first nine predicted buckling loads are reported in Table 2.

| Method | Element size | Buckling mode | | | | | | | | |
|---|---|---|---|---|---|---|---|---|---|---|
| | | 1 | 2 | 3 | 4 | 5 | 6 | 7 | 8 | 9 |
| Present | 0.005 m | 18.122 | 93.933 | 271.33 | 418.66 | 455.50 | 764.19 | 791.48 | 917.11 | 994.67 |
| | 0.0025 m | 17.984 | 91.723 | 255.49 | 375.17 | 422.26 | 710.01 | 710.88 | 825.61 | 892.06 |
| | 0.00125 m | 17.923 | 91.057 | 251.12 | 364.37 | 413.41 | 685.82 | 694.39 | 801.73 | 856.76 |
| ABAQUS (S4) [6] | Element number | 17.9435 | 93.7975 | 269.975 | 418.400 | 452.825 | - | - | - | - |
| XSHELL [6] | 200 | 18.148 | 94.0725 | 272.200 | 420.725 | 456.975 | - | - | - | - |

Table 2: Convergence study on linear buckling loads of delaminated plate ($t$=40 mm).

A fair convergence property is achieved for the model containing extra DOFs. The obtained results are closer to the ones of ABAQUS (S4) standard element in where the delaminated region was simulated through defining double nodes. The corresponding first and fourth mode shapes of the finest mesh scheme are depicted in Figure 5. All post-processing concerning the delaminated state is performed in the standard postprocessor of ANSYS by creating virtual elements and assigning results obtained from extra dofs to them.

Next, the length of the delamination is altered to 45 mm and 50 mm and the first nine buckling loads are compared in Table 3. The element size for the present model is supposed to be 0.00125 m.

| $t$ (mm) | Method | Buckling mode | | | | | | | | |
|---|---|---|---|---|---|---|---|---|---|---|
| | | 1 | 2 | 3 | 4 | 5 | 6 | 7 | 8 | 9 |
| 45 | Present | 17.331 | 80.522 | 214.04 | 282.01 | 392.91 | 562.48 | 635.95 | 714.14 | 725.66 |
| | XSHELL [6] | 17.937 | 90.702 | 256.900 | 390.730 | 446.800 | - | - | - | - |
| 50 | Present | 16.634 | 72.425 | 182.85 | 224.15 | 372.36 | 458.72 | 595.60 | 640.83 | 649.24 |
| | XSHELL [6] | 16.850 | 74.378 | 196.450 | 242.790 | 410.500 | - | - | - | - |

Table 3: Buckling loads of composite plates with delamination ($t_1$=45 mm and $t_2$=50 mm).

As it was expected, by increasing the delaminated area the predicted buckling loads are reduced. The calculated buckling loads, especially the fundamental ones, are in a good agreement with Ref [6].

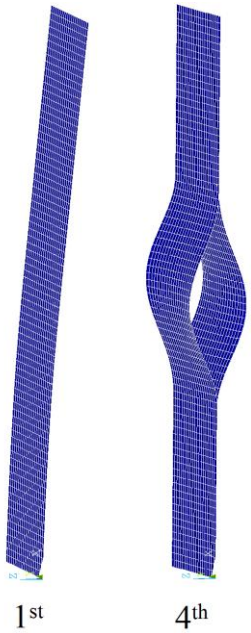


Figure 5: Linear buckling mode shapes of delaminated composite plate ($t$=40 mm).

In the final example, the non-linear buckling analysis of the previous plate is carried out. In order to enable tracking the post-buckling response of the laminate under compressive load condition, very small imperfection amplitudes has been utilized. In the present XFEM formulation we are restricted to only one middle plane, even for discontinuous regions. Therefore, the application of geometric imperfection for the aforementioned problems is not provided. Void layers of variable thickness as well as non-zero initial jumps for the $z$-coordinates of the upper region had been under discussion to get stress-free imperfections but finally a force-type perturbation was chosen. This type of imperfection is applied in literatures to the discontinuous layers when the plate with delamination under compression is investigated. This method can be effectively implemented in the XFEM topology through the availability of the extra DOFs. Herein, a new algorithm which describes a method to apply forces leading to a deformation proportional to the buckling mode has been applied. The flowchart view of this algorithm is shown in Figure 6. The proposed method is applied to ANSYS version 14.5 commercial software.

The algorithm is started with performing a linear buckling analysis. By depicting the linear buckling mode shapes, one can identify whether the critical load corresponds to the local delamination mode shape or not. If so, a factor of dislocations is utilized in the form of displacement constraints to retrieve the nodal reaction forces in a linear static analysis. Next, the force values of the extra DOFs are applied to the discontinuous section of model and the non-linear analysis is initiated in its first step. By doing so, the deformations proportional to that buckling mode are calculated. Thereafter, the same analysis is being continued after applying compressive loads. It is noted that when the linear buckling analysis of laminates with discontinuity is carried out, the critical buckling mode shape is not necessarily represents the local delamination mode shape. Therefore, one further step is required to include the geometrical

imperfection from the critical buckling mode shape. By following the above algorithm, the possibility of opening multi bifurcation paths is provided.

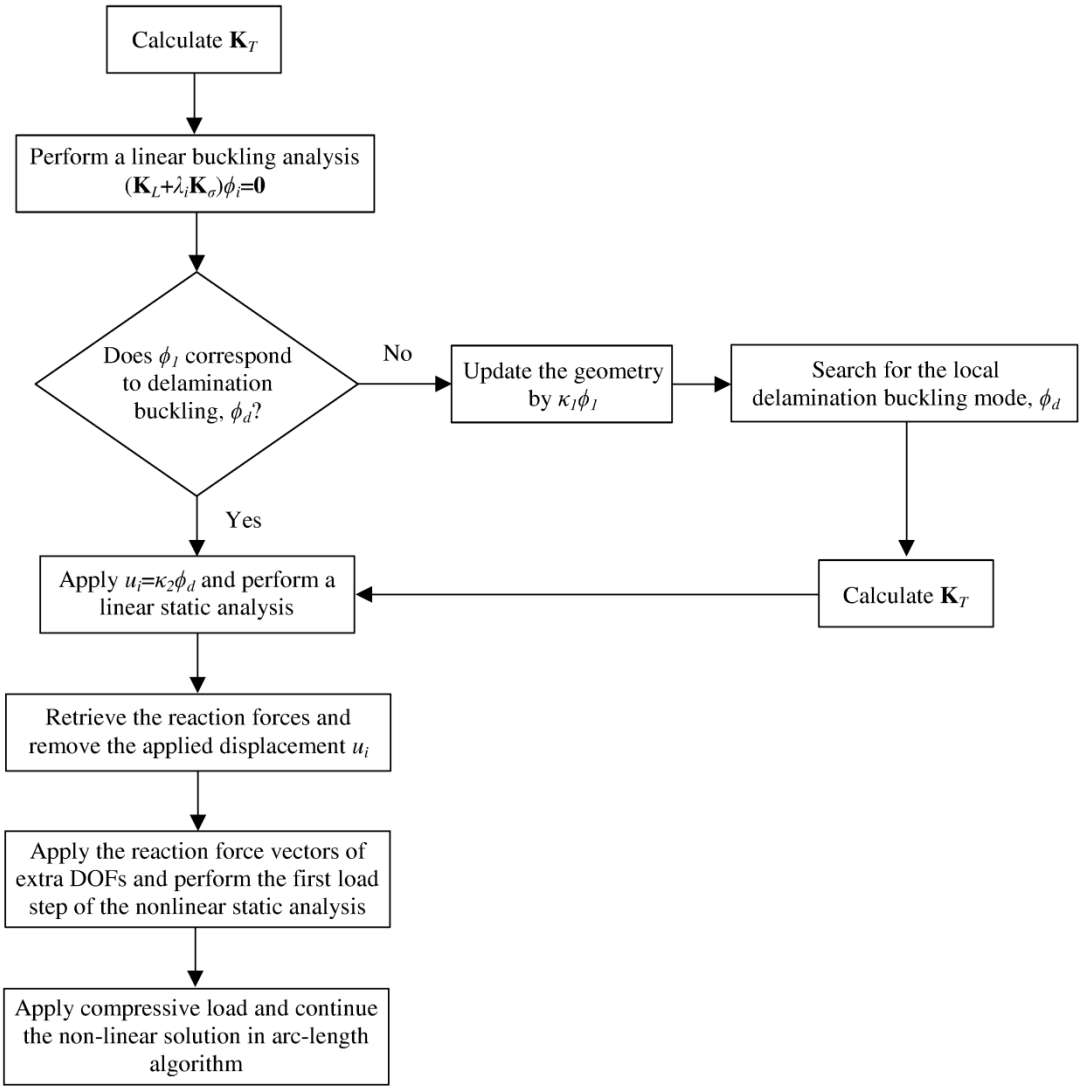


Figure 6: Flowchart of the non-linear delamination buckling analysis.

In the previous linear buckling study, the critical buckling mode was associated to the bending of the structure whereas the fourth one was corresponded to the outward separation of layers. Therefore, in order to carefully track the response of the laminate, a combination effect of the mode I and IV is considered. The amplitudes of imperfections are assumed as $\kappa_1=h$ and $\kappa_2=0.025h$. It should be mentioned that excluding the bending imperfection will lead to negative pivot values in the vicinity of the critical buckling load. The element size is supposed to be 1.25 mm. The load versus the transverse displacement of the edge in where the compressive load was applied is compared with the undamaged one in Figure 7.

A meaningful reduction of the maximum carried load is observed for the laminated plates containing the greater delaminated surface. Moreover, higher load magnitudes are supported by the undamaged plate than the delaminated ones. Taking the results of the linear buckling analysis as the reference, the maximum supported load for the undamaged laminate is close to the critical one. However, less load amplitudes was supported by the delaminated ones.

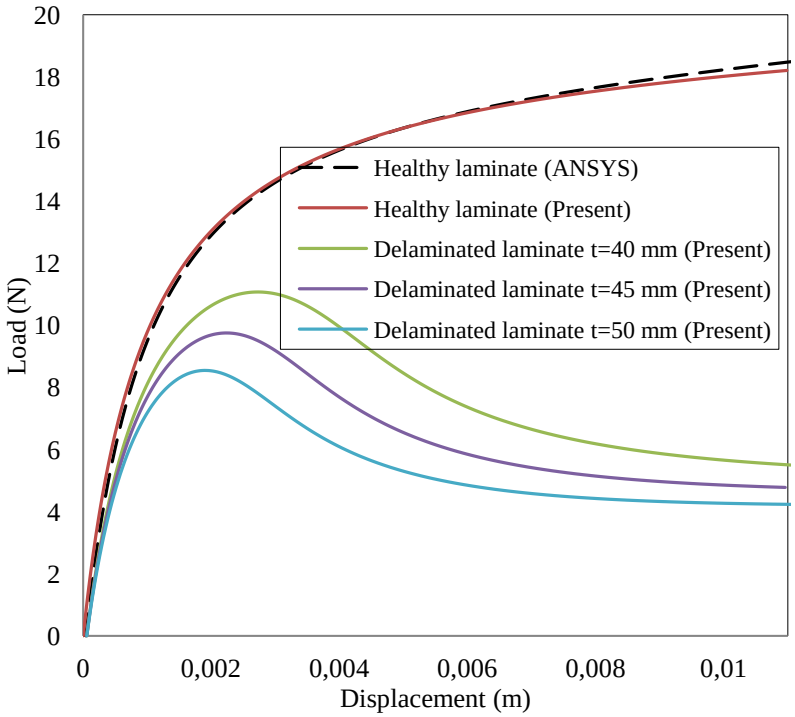


Figure 7: Axial load versus transverse displacement of composite laminated plate under compressive load.

The deformed shape of the composite laminates with delamination $t$=40 mm at the last load step is shown in Figure 8.

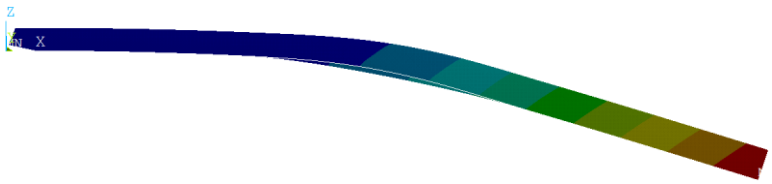

Figure 8: Deformed shape of the composite laminated plate with delamination under compressive load.

## 4 DELAMINATION INITIATION AND PROPAGATION

The danger of delamination is checked by a stress criterion based on interlaminar shear and normal stress obtained from equilibrium. However, the determination of interlaminar shear stress requires the derivative of in-plane normal stress which is constant in a low order element. Therefore, nodal averaging of in-plane stress is carried out before forming the derivative.

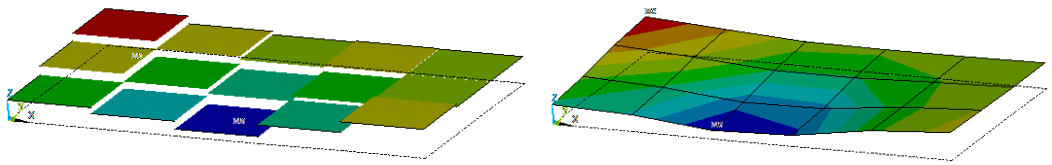

Figure 9: Elemental and averaged stress.

Furthermore, interlaminar normal stress is in equilibrium with the change of transverse shear stress, requiring another derivative. This can deteriorate the accuracy. In the example shown in Figure 10 this mainly holds for the normal stress.

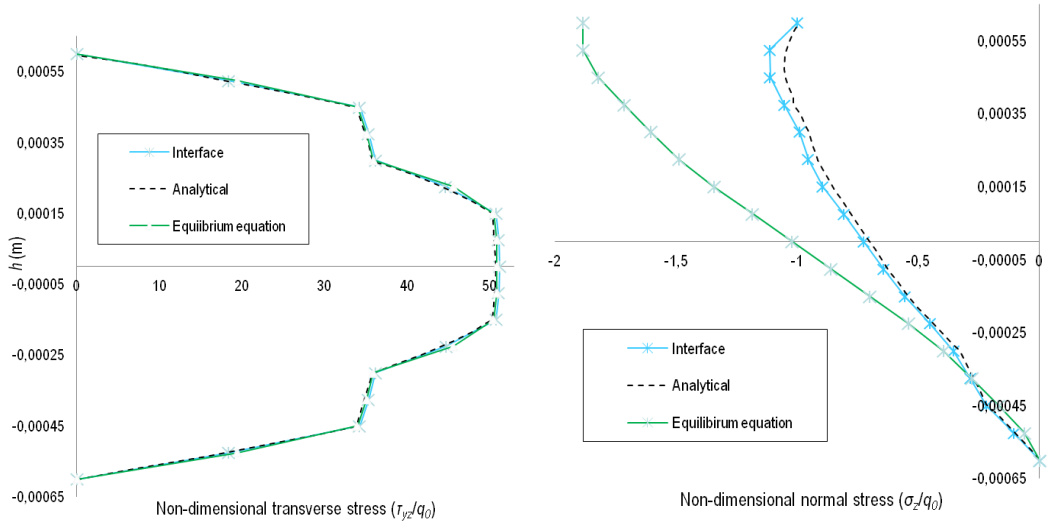


Figure 10: Shear- and out-of-plane normal-stress distribution, comparison of interfacial stress and stress from equilibrium with analytical solution from [9].

The simulation of delamination propagation with this XFEM shell element including a mixed-mode cohesive-zone model and the influence of the integration scheme has been presented by the authors e.g. in [8]. The relative displacements in the interface between lower an upper part are directly obtained from the extra dofs $a_i$ multiplied by the element shape functions. Instead of using a stress-strain relation the interfacial stress depends on the relative motion. Hence, this stress distribution is continuous over the element edges and one order higher than that from strain anywhere else in the finite element. All interfacial stress components are available from the cohesive model. Therefore, for delamination initiation and propagation the algorithm is as follows:

- start with continous model – one element over the thickness for all layers
- at certain load levels
  - calculate interlaminar stress from equilibrium between all layers
  - evaluate the delamination criterion
  - if the criterion indicate danger of delamination at a certain location set the element and its neighborhood to discontinuous and introduce the interfacial cohesive model
- continue with loading

## 5 CONCLUSIONS

The delamination buckling analysis of composite laminates is investigated. Thus, a new XFEM model based on a lower order laminate theory is developed. In the present approach, the formulation is enhanced by adding extra DOFs; and subsequently, the delaminated surface can be described by only one four-noded element. Therefore, no extra element are needed to simulate the subdomains. Moreover, the definition of contact element and imperfections for the post-buckling analysis are facilitated through the available enriched DOFs. The performance of the model is successfully verified with the available results in literature.

## REFERENCES


[1] N. Moës, J. Dolbow, T. Belytschko, A finite element method for crack growth without remeshing. *International Journal of Numerical Methods in Engineering*, **46.1**, 131-150, 1999.

[2] P. Wriggers, *Nonlinear finite element methods*. Springer Science & Business Media, 2008.

[3] E. Oñate, *Structural Analysis with the Finite Element Method. Linear Statics: Volume 2: Beams, Plates and Shells*. Springer, 2013.

[4] O.C. Zienkiewicz, R.L. Taylor, *The finite element method, Vol. 2: Solid Mechanics, 5th Edition*. McGraw Hill, 2000.

[5] K.Y. Sze, X.H. Liu, S.H. Lo, Popular benchmark problems for geometric nonlinear analysis of shells. *Finite elements in analysis and design*, **40.11**, 1551-1569, 2004.

[6] T. Nagashima, H. Suemasu, X-FEM analyses of a thin-walled composite shell structure with a delamination. *Computers & structures*, **88.9**, 549-557, 2010.

[7] W. Rust, *Non-linear Finite Element Analysis in Structural Mechanics*. Springer, 2015.

[8] S. Yazdani, W.J.H. Rust, P. Wriggers, *An XFEM approach for modelling delamination in composite laminates*, Composite Structures (2016), pp. 353-364

[9] T.B. Hartman, M.W. Hyer, S.W. Case, Stress Recovery in Composite Laminates. In: *52nd AIAA/ASME/ASCE/AHS/ASC Structures, Structural Dynamics and Materials Conference*, Denver, Colorado; 4–7 April 2011.